

# Doping-induced metallicity and coexistence of magnetic subsystems in $\text{K}_2\text{Fe}_{4+x}\text{Se}_5$

Liqin Ke,<sup>1</sup> Mark van Schilfgaarde,<sup>2</sup> and Vladimir Antropov<sup>1</sup>

<sup>1</sup>*Ames Laboratory USDOE, Ames, IA 50011*

<sup>2</sup>*Department of Physics, King's College London*

(Dated: November 14, 2018)

Electronic structure calculations are used to analyze the electronic and magnetic properties in  $\text{K}_2\text{Fe}_{4+x}\text{Se}_5$ . Fe atoms can be divided into two distinct groups. The  $x=0$  (parent) compound forms an insulating, collinear, local moment phase with high Néel temperature. We show that large bi-quadratic exchange coupling and exchange-elastic interactions stabilize the magnetic order. For  $x>0$  the additional Fe atoms fill vacancy sites. They form impurity bands for small  $x$ , which broaden as  $x$  increases. They determine the states at the Fermi level and may be viewed as a magnetic subsystem separate from the host. Spin fluctuations are prevalent because magnetic interactions between the ‘defect’ and the ‘parent’ atoms are relatively weak, while chemical fluctuations are prevalent for low  $x$ . Fluctuations of either type leads to the formation of a weakly metallic state. The unusual coexistence of the two magnetic subsystems offers a new perspective as to how superconductivity and strong antiferromagnetism can coexist. We argue that spin fluctuations of the impurity subsystem share common features with the Fe-pnictide superconductors.

PACS numbers: PACS number

The iron selenide superconductors  $\text{K}_2\text{Fe}_{4+x}\text{Se}_5$  discovered recently<sup>1</sup>, demonstrate superconducting properties similar to their pnictide counterparts, even though they appear to have very different magnetic ordering<sup>2</sup> (compare Figs. 1a, 1b) and electronic structure near the Fermi level  $E_F$ <sup>3</sup>. This has a bearing on the associations made between particular characteristics found in the pnictides, whose properties are largely invariant from one material to another, to the superconductivity observed. Spin interactions are likely to play a key role in mediating superconductivity; yet their character is not yet well understood<sup>4</sup>. While biquadratic exchange coupling<sup>5</sup> makes possible a consistent description of magnetism in pnictides which form the striped antiferromagnetic (AFM) ground state (Fig. 1b), it is not clear what interactions are responsible for the stabilization of the unusual magnetic structure observed in selenides<sup>2</sup> (Fig. 1a). In addition, while weak (and most likely itinerant) AFM ( $T_N \sim 30\text{--}40\text{K}$ ) and weak superconductivity ( $T_c \sim 1\text{--}10\text{K}$ ) have been observed to coexistence in the pnictides<sup>4</sup>, the situation is altered in this material. Magnetic moments and Néel temperature are much larger, strongly favoring the local moment picture, and the coexistence of AFM with superconductivity is much more robust ( $T_N \sim 640\text{K}$  and  $T_c \sim 30\text{K}$ )<sup>2,6,7</sup>.

In spite of these differences, we will explain how it comes about that  $\text{K}_2\text{Fe}_{4+x}\text{Se}_5$  is metallic, how these two families share some key features in common, and further how these common characteristics can potentially provide a framework to explain why these quite distinct material classes show similar superconductivity, while having quite different kinds of magnetic interactions. If such an hypothesis is correct, this work elucidates what the essential elements are for superconductivity to appear.

The crystalline and magnetic structure of the parent compound  $\text{K}_2\text{Fe}_4\text{Se}_5$  have been studied in Ref.<sup>8</sup>. Vacancies substitute for 20% of the Fe sites in the unusual

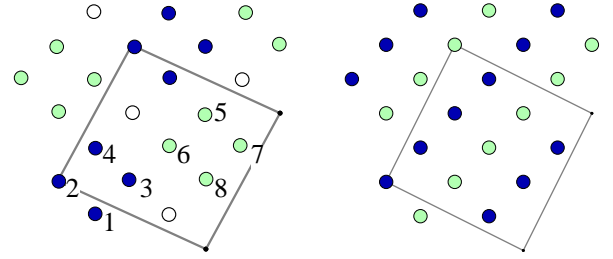


FIG. 1: Magnetic configuration of  $\text{K}_2\text{Fe}_{4+x}\text{Se}_5$  in the block Néel structure. Parallelepiped shows unit cell. Fe atoms in the  $xy$  plane are shown: dark (blue) and light (green) depict spin-up and spin-down Fe atoms, respectively. There is a slight distortion of the square (sites 1-4), elongating (shortening) the diagonal along  $x$  ( $y$ ). Open circles depict 4d sites that are empty for  $x=0$ , but get populated as  $x$  increases. Relaxation significantly stabilizes the magnetic order. Right panel shows same atoms in the striped AFM configuration found in the Fe pnictides, with  $x=1$ .

ordered superstructure shown in Fig. 1a. The Fe are arranged in squares of four atoms in a block with the spins parallel. The blocks themselves are aligned antiferromagnetically, with two layers of atoms depicted in the Figure.  $\text{K}_2\text{Fe}_4\text{Se}_5$  has been identified as a magnetic semiconductor<sup>2,6,8,9</sup>, with the Fe local moment observed to be  $\sim 3\mu_B$ . It has been argued that superconductivity appears in this system as a result of vacancy formation<sup>2,6,8,9</sup>.

For the parent system  $\text{K}_2\text{Fe}_{4+0}\text{Se}_5$ , our (LDA) calculation predicts a magnetic semiconductor in the block Néel structure with a local moment  $M=2.9\mu_B$  and a bandgap of 0.44 eV, confirming the experiment and the findings of a prior study<sup>8</sup>. This latter work also concluded that lattice relaxation is necessary to stabilize the block Néel magnetic structure. We use the lattice constants of that work; our LDA implementation is described in Ref.<sup>10</sup>.

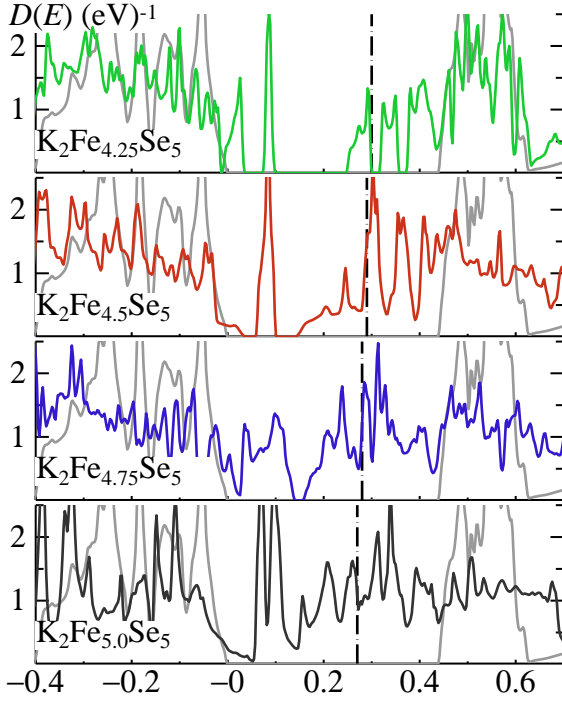


FIG. 2: Total DOS per Fe atom of  $K_2Fe_{4+x}Se_5$  in the collinear block Néel structure, for  $x=0.25, 0.5, 0.75$  and at  $x=1$  where all Fe vacancies are filled. The parent compound ( $x=0$ ) is drawn in light grey, with a gap of 0.44 eV and the VBM aligned to 0. The remaining DOS are approximately aligned to the parent compound;  $E_F$  is drawn as a vertical dot-dashed line for each panel. As Fe begins to populate the vacancy sites (top panel), three distinct, very narrow bands appear between 0.25 and 0.4 eV;  $E_F$  lies between the first and second. Another localized state appears at  $E=0.08$  eV, and the VBM of the parent compound, splits. As  $x$  increases from 0.25 to 0.5, the midgap states (especially the state just below  $E_F$ ) broaden but begin to overlap, and when  $x=0.75$  they merge with the host bands.

We consider how populating vacancy sites with Fe atoms affects the electronic spectrum and metallicity of the system, constrained for now to be in a collinear magnetic configuration. We denote Fe atoms in the parent compound as 16i atoms, and those filling the vacancy sites as 4d atoms, following customary nomenclature. Supercells of the parent structure were generated, and a subset of the vacancy sites populated. In each case the lattice was relaxed to its minimum-energy configuration, using the PBE functional. (PBE-relaxed bond lengths, are in better agreement with experiment LDA ones; the average Fe-Se bond length in  $K_2Fe_{4+0}Se_5$  is 2.444 Å, close to the reported value. But we use PBE only to relax the structure; the LDA is preferred for magnetic interactions.) Fig. 2 compares the evolution of total DOS  $D(E)$ , with  $x$  against the parent compound,  $x=0$ . For  $x=0.25$ , a pair of localized states form in the gap: the lower band is filled and the upper band is empty. Both states broaden as  $x$  increases to 0.5; still they are nearly separated so that the system is at best weakly metallic (keeping in mind

the LDA tends to overestimate hybridization and bandwidths). Magnetic moments range from 2.1–2.3  $\mu_B$  (Fe on 4d sites) to 2.7–2.9  $\mu_B$  (16i sites) at  $x=0.25$ . Thus in the absence of any fluctuations the impurity band widens, inducing a transition from semiconducting ( $D(E_F)=0$ ) to weakly metallic behavior for  $x \gtrsim 0.25$ .

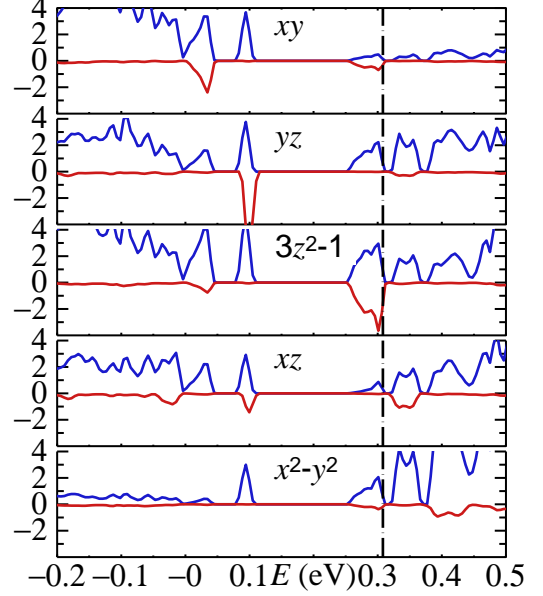


FIG. 3: Site and  $m$ -resolved  $d$  partial DOS  $D(E)$  per Fe atom in  $K_2Fe_{4.25}Se_5$ .  $E_F$  is shown as a vertical line: the energy zero is chosen to align with the VBM of  $K_2Fe_4Se_5$ .  $D(E)$  above the zero line are the  $m$ -resolved DOS summed over the 32 Fe 16i sites, while DOS below the zero line are summed over the two Fe 4d sites. The defect state slightly above  $E_F$  is confined to the host sites, while the one just below  $E_F$ , of  $3z^2-1$  character, is centered on the 4d site, with tails extending to the host.

In Fig. 3  $D(E)$  is resolved onto  $m$  components of  $d$  partial waves at the 4d and 16i Fe sites. The occupied defect band just below  $E_F$  is centered on the Fe 4d  $3z^2-1$  orbital, with tails penetrating into the host whose cumulative weight approximately matches the head. The empty band, on the other hand, is almost completely confined to the host sites, and is analogous to a “surface” resonance.

It is apparent that *chemical disorder* of Fe 4d atoms will lead to strong fluctuations in the local  $D(E_F)$ : in regions where locally  $x > 0.5$  defect bands will overlap and the system will be locally metallic. If the vacancy occupation is random the local site occupation (concentration) will follow a binomial distribution, which can be reasonably approximated by a Gaussian distribution. Then the probability  $P$  of finding a composition fluctuation in a region containing  $N$  ions with amplitude exceeding  $\Delta x_{\min}$  can be written in terms of the standard deviation  $\sigma$  as

$$P(\Delta x_{\min}; x; N) = \text{erfc} \left( \Delta x_{\min} / \sqrt{2\sigma^2} \right) \quad (1)$$

where  $\sigma^2 = x(1-x)/N$ . The defect wave functions are sufficiently short ranged that a sphere containing about

8 vacancy sites are sufficient to stabilize the local DOS. Partitioning an a compound with  $x=0.25$  average vacancy occupation into overlapping spheres of 8 vacancy sites each, about 10% of the spheres would contain a local concentration of  $x>0.5$ . Thus from percolation theory we can expect sizable portions of metallic behavior even at  $x=0.25$ , owing merely to local fluctuations in the concentration of 4d Fe atoms.

Perhaps more important, there will be strong spin fluctuations on the 4d Fe sites, as we describe below. The 16i and 4d Fe atoms contribute to the electronic structure in approximately independent ways. The former have large local moments, are strongly exchange-coupled as described below, and form an insulating block magnetic Néel structure. They form relatively wide  $d$  bands with a large DOS; however, their contribution to the DOS is shifted away from  $E_F$ . Addition of 4d atoms causes defect levels to appear in the bandgap, which weakly couple to the 16i atoms to form a narrow defect band or resonance, at  $E_F$ . Though local moments of these atoms are calculated to be  $2.3\mu_B$  their magnetic coupling to the host is weak. The reason is as can be seen in Fig. 1a, in a collinear configuration, spins at the 4d sites must align parallel to one neighboring block and antiparallel to the other. The exchange field from the two blocks nearly cancel, so the net exchange at these sites is weak. Therefore large, low-energy spin fluctuations must result. Such fluctuations can strongly reduce or even kill the Fe 4d static magnetic moment, making the 4d subsystem paramagnetic. This subsystem is thus similar to the entire lattice in other superconductors such as LiFeAs and FeSe. In such materials band theory predicts stable and large moment while experiment clearly shows it is not present. In two recent Mössbauer studies<sup>11,12</sup> ‘nonmagnetic’ Fe atoms were observed to coexist with the magnetic ones, e.g. in Ref. 11, 15% of Fe atoms in a  $\text{K}_2\text{Fe}_{4+0.4}\text{Se}_5$  sample were reported to be nonmagnetic.

There are a host of recent experiments<sup>2,13</sup> demonstrating that antiferromagnetism and superconductivity coexist. This has prompted considerable debate in the literature as to whether the two effects are present in the same phase, or whether a separate phase coexists that is responsible for superconductivity. Several works present experimental evidence for a second phase; see e.g. Ref.<sup>14</sup>. It is suggested that one phase is insulating in the block magnetic Néel structure that carries the antiferromagnetism, and the other in a nonmagnetic phase similar to FeSe, that carries the superconductivity. There appears to be contradictory experimental evidence for both the “one-phase” and “two-phase” scenarios.

The present work cannot rule out either scenario. But our findings show how it is possible that magnetism and superconductivity can coexist in a single phase. The 4d Fe atoms generate a rather itinerant channel or subsystem of states at  $E_F$  largely decoupled from the 16i magnetic structure. Fluctuations on the 4d subsystem will be large and the system as a whole weakly metallic even for small  $x$  as a consequence of spin (and chemical)

TABLE I: Average values of first and second NN exchange couplings,  $\bar{J}_1$  and  $\bar{J}_2$ , in meV, for  $\text{K}_2\text{Fe}_4\text{Se}_5$ . Interblock couplings are indicated with a prime, while intrablock couplings are unprimed. Also shown are the Néel temperature, estimated in the mean-field and random-phase approximations.

	$M$	$\bar{J}_1$	$\bar{J}_2$	$\bar{J}'_1$	$\bar{J}'_2$	$T_N^{MFA}$	$T_N^{RPA}$
unrelaxed	2.9	-5.7	17.0	25.7	6.7	682	—
relaxed	2.9	-9.7	10.2	27.3	8.5	944	494

disorder. Separation of the 4d and 16i magnetic subsystems is clear, as we show below, but the electronic states are somewhat mixed and eigenstates at  $E_F$  have projections onto both 4d and 16i atoms (Fig. 3). Thus superconducting pairing still can originate from electrons of both subsystems, even while the metallic state is established by the small fraction of 4d Fe atoms, in a spin (and chemically) disordered configuration.

Next we study the exchange coupling by using a Green’s function linear-response technique, as described in Ref.<sup>15</sup>. Average values for such linear response  $\bar{J}$  are shown in Table 1 for both ideal and relaxed  $\text{K}_2\text{Fe}_4\text{Se}_5$  structures. Exchange interactions more distant than second neighbor are found to be small, and we present only NN and 2NN parameters. We distinguish between intrablock couplings between FM aligned neighbors ( $\bar{J}_1$ ,  $\bar{J}_2$ ) and interblock couplings between AFM aligned neighbors ( $\bar{J}'_1$ ,  $\bar{J}'_2$ ). Relaxation stabilizes the magnetic order, as can be seen by inspection of the individual  $\bar{J}$ ’s or from the Néel temperature estimated in the mean field and RPA approximations (Table 1).

$\bar{J}_1$  and  $\bar{J}'_1$  are radically different. This calls into question the customary interpretation of these parameters in terms of the Heisenberg model. We can extend the Heisenberg hamiltonian to include biquadratic terms, and assume<sup>5</sup> that

$$H = \sum_{ij} \bar{J}_{ij} \mathbf{S}_i \cdot \mathbf{S}_j; \quad \bar{J}_{ij} = J_{ij} - 2K_{ij} \mathbf{S}_i \cdot \mathbf{S}_j. \quad (2)$$

For small angles, where linear response is applicable,  $K_{ij}$  can be eliminated if the intrablock and interblock  $J_{ij}$  are permitted to be different. It is apparent from the reduced symmetry that  $J$  need not be  $J'$ ; moreover for small angles the anisotropic Heisenberg and biquadratic models are not distinguishable. They can only be distinguished at large angles; thus we evaluate the biquadratic term explicitly through calculations of the total energy  $E$  in large-angle noncollinear configurations. We accomplish this in practice by rotating the orientation of four atoms surrounding to one vacancy in a unit cell relative to the four surrounding the other vacancy (Fig. 1a), by a series of angles  $\theta$  ranging between 0 and  $\pi$ . Because this particular rotation preserves all second-neighbor angles, only NN terms in Eq. (2) contribute. A Fourier transform of  $E(\theta)$  yields directly the sum of all pairwise terms in Eq. (2), i.e.  $J = \sum_{ij} J_{ij}$ ,  $K = \sum_{ij} K_{ij}$  and terms higher order in  $\cos(\theta)$ . Terms beyond the biquadratic are found to be small, so only  $J$  and  $K$  need be con-

sidered. As a check,  $J + 2K$  calculated this way should match  $\bar{J} = \sum_{ij} \bar{J}_{ij}$  calculated by linear response. Indeed we find this to be the case: the two calculations agree to within 3%. A large biquadratic coupling  $K_{ij}$  of positive sign, on the same order as  $J_{ij}$ , is necessary to explain the anisotropy in  $\bar{J}$  and  $\bar{J}'$ . This system is best characterized by large positive biquadratic coupling, which initially affects AFM coupling between blocks and FM coupling inside them.

Lattice relaxation (which depends on  $x$ ) stabilizes FM coupling inside blocks, as can be seen by its effect on  $\bar{J}_1$ , Table 1. FM coupling is further stabilized by local distortions originating from partial filling of the 4d Fe sites. Bilinear and biquadratic exchange interactions both change with relaxation, even while magnetic moment amplitudes are nearly constant. This effect, which we term the “exchange-striction” effect analogous to the well-known magnetostriction, is in part responsible for stabilizing the observed magnetic ground state.

The magnetic structure and electronic states at  $E_F$  in iron selenides appear to be very different from the Fe pnictides. Nevertheless they share in common a large biquadratic coupling, which in each case helps to stabilize the magnetic ground state structure. In  $\text{K}_2\text{Fe}_{4+x}\text{Se}_5$  this mechanism is further affected by strong ‘exchange-striction’. We showed that two nearly independent subsystems coexist: a strong AFM phase with large local moments and high Néel temperature, and a more itiner-

ant phase with fluctuating moments. Further, the metallic state (a prerequisite for superconductivity) is a consequence of fluctuations. This creates a plausible scenario to explain the coexistence of superconductivity and strong AFM observed in a single phase. In addition, both pnictides and selenides share two key generic properties: antiferromagnetic interactions create a pseudogap in both cases, and the DOS at  $E_F$  is relatively low. This is also a prerequisite for spin-mediated superconductivity because a large DOS at  $E_F$  can be a major source of incoherent spin scattering, which is usually destructive to superconductivity originating from spin fluctuations. The large moments we find on the 4d subsystem is likely an artifact of density functional theory — a mean field approach which does not incorporate fluctuations, and is expected to be very similar to the well known overestimate of the static magnetic moment in many iron pnictides systems. Thus the appearance of such soft ‘itinerant’ magnetic elements with weakly magnetic or paramagnetic spin fluctuations can be considered as the only generic feature of both iron pnictides and chalcogenides, while detailed electronic structure near the Fermi level, shape of the Fermi surface, magnetic structures and symmetry of superconducting order parameter seems not universal and not generic.

Work at the Ames Laboratory was supported by US DOE Basic Energy Sciences, Contract No. DE-AC02-07CH11358

- 
- <sup>1</sup> J. Guo, S. Jin, G. Wang, S. Wang, K. Zhu, T. Zhou, M. He, and X. Chen, *Phys. Rev. B* **82**, 180520 (2010).
  - <sup>2</sup> W. Bao, Q.-Z. Huang, G.-F. Chen, M. A. Green, D.-M. Wang, J.-B. He, and Y.-M. Qiu, *Chin. Phys. Lett.* **28**, 086104 (2011).
  - <sup>3</sup> Y. Zhang, L. X. Yang, M. Xu, Z. R. Ye, F. Chen, C. He, H. C. Xu, J. Jiang, B. P. Xie, J. J. Ying, et al., *Nature Mater.* **10**, 273 (2011); T. Qian, X.-P. Wang, W.-C. Jin, P. Zhang, P. Richard, G. Xu, X. Dai, Z. Fang, J.-G. Guo, X.-L. Chen, et al., *Phys. Rev. Lett.* **106**, 187001 (2011).
  - <sup>4</sup> D. C. Johnston, *Advances in Physics* **59**, 803 (2010).
  - <sup>5</sup> A. L. Wysocki, K. D. Belashchenko, and V. P. Antropov, *Nature Phys.* **7**, 485 (2011).
  - <sup>6</sup> P. Zavalij, W. Bao, X. F. Wang, J. J. Ying, X. H. Chen, D. M. Wang, J. B. He, X. Q. Wang, G. F. Chen, P.-Y. Hsieh, et al., *Phys. Rev. B* **83**, 132509 (2011).
  - <sup>7</sup> R. H. Liu, X. G. Luo, M. Zhang, A. F. Wang, J. J. Ying, X. F. Wang, Y. J. Yan, Z. J. Xiang, P. Cheng, G. J. Ye, et al., *EPL (Europhysics Letters)* **94**, 27008 (2011).
  - <sup>8</sup> X.-W. Yan, M. Gao, Z.-Y. Lu, and T. Xiang, *Phys. Rev. Lett.* **106**, 087005 (2011); C. Cao and J. Dai, *Phys. Rev. Lett.* **107**, 056401 (2011).
  - <sup>9</sup> W. Bao, G. N. Li, Q. Huang, G. F. Chen, J. B. He, M. A. Green, Y. Qiu, D. M. Wang, and J. L. Luo, *ArXiv e-prints* (2011), 1102.3674.
  - <sup>10</sup> T. Kotani and M. van Schilfhaarde, *Phys. Rev. B* **81**, 125117 (2010).
  - <sup>11</sup> D. H. Ryan, W. N. Rowan-Weetaluktuk, J. M. Cadogan, R. Hu, W. E. Straszheim, S. L. Bud’ko, and P. C. Canfield, *Phys. Rev. B* **83**, 104526 (2011).
  - <sup>12</sup> V. Ksenofontov, G. Wortmann, S. A. Medvedev, V. Tsurkan, J. Deisenhofer, A. Loidl, and C. Felser, *Phys. Rev. B* **84**, 180508 (2011).
  - <sup>13</sup> F. Ye, S. Chi, W. Bao, X. F. Wang, J. J. Ying, X. H. Chen, H. D. Wang, C. H. Dong, and M. Fang, *Phys. Rev. Lett.* **107**, 137003 (2011); A. M. Zhang, J. H. Xiao, Y. S. Li, J. B. He, D. M. Wang, G. F. Chen, B. Normand, Q. M. Zhang, and T. Xiang, *ArXiv e-prints* (2011), 1106.2706.
  - <sup>14</sup> A. Ricci, N. Poccia, G. Campi, B. Joseph, G. Arrighetti, L. Barba, M. Reynolds, M. Burghammer, H. Takeya, Y. Mizuguchi, et al., *Phys. Rev. B* **84**, 060511 (2011).
  - <sup>15</sup> M. van Schilfhaarde and V. P. Antropov, *J. Appl. Phys.* **85**, 4827 (1999).